

Simple calculations of confinement states in a quantum well

M. F. H. Schuurmans and G. W. 't Hooft

Philips Research Laboratories, P.O. Box 80000, 5600 JA Eindhoven, The Netherlands

(Received 26 September 1984)

A simple and unified description of conduction- and valence-band confinement states in a quantum well is developed. In particular, the lowest confinement states in GaAs/Ga_{1-x}Al_xAs ($0 \leq x \leq 1$) are accurately described. From a detailed comparison with a much more involved, 20-band, tight-binding description, the accuracy is estimated to be better than a few percent in the confinement energies. The description is easily numerically implemented.

I. INTRODUCTION

The present paper aims at a simple, precise, and unified model description of conduction- and valence-band confinement states in a quantum well. Our main interest is GaAs/Ga_{1-x}Al_xAs, but the model may also be applied to other quantum wells where charge transfer across the interface is irrelevant, i.e., to type-I quantum wells. In the past several models have been proposed for the description of these states. Dingle¹ has used a simple "particle in the box" description with different effective masses for the particle in the well and in the barrier and with a confinement potential determined essentially by the different electron affinities of the well and barrier materials. The model is physically appealing because of its simplicity and transparency. It has been used by Mukherji and Nag² and, more recently, by Vojak *et al.*³ to describe the GaAs/Ga_{1-x}Al_xAs quantum well.

A most elaborate description of confinement in a quantum well has been given recently by Schulman and Chang.⁴ They describe the complex band structure of the well and barrier materials using an *s,p,s** nearest-neighbor empirical tight-binding model.⁵ The confinement states are obtained by expansion in terms of the well and barrier eigenstates at the confinement energy. The method is in our opinion the most precise existing semiempirical description of confinement. A comparison of the results of the simple Dingle model and the elaborate Chang-Schulman model shows that the simple model is only applicable for very small confinement energies, i.e., for large well widths and/or small potential steps. This is still true⁶ if the incorrect envelope derivative continuity in this model is replaced by the more appropriate continuity condition as derived by White and Sham⁷ and Bastard.⁸ Apparently the simple model is too simple. A model of intermediate complexity is due to Bastard.⁹ It uses a Kane¹⁰ envelope function description involving six bands (including spin): two bands describe the bottom of the conduction band and four bands describe the top of the valence band. The spin-orbit split-off band is disregarded as well as, except for the heavy holes, the coupling to other bands and the free-electron dispersion part. The latter effects are included by Altarelli,¹¹ but the split-off band is still disregarded. Indeed the description is mainly intended for the quantum wells InAs/GaSb and HgTe/CdTe, where the spin-orbit splitting is large, and not for

GaAs/Ga_{1-x}Al_xAs, our main interest. A further disadvantage of the Bastard⁹ approach is that only one adjustable parameter is available to describe the electron (el) and light-hole (lh) bands; the parameter is the matrix element of the momentum operator between a top valence-band state and the bottom conduction-band state. As a consequence this parameter must be given different values to describe the different effective masses in the el and lh bands. The approach by Altarelli,¹¹ containing more adjustable parameters relating to the coupling with other bands, *does* give a unifying description of these bands.

In this paper we present a simple Kane-type model which includes the el, lh, heavy hole (hh) and spin-orbit split-off (so) band and, perturbatively, the coupling to the other bands. The model contains for each material, four adjustable coupling parameters which are fixed by the el, lh, hh, and so effective masses in the Γ point. A unified description of the dispersion of the four bands is thereby achieved. The model is then further simplified. For the el and hh confinement a Dingle-type particle in the box description is derived. However, the el effective masses in well and barrier will be energy dependent according to our Kane model. For the lh confinement, a similar description pertains unless the confinement energies become comparable to the spin-orbit splitting. In the latter case we use a simple Kane-type model in which only the lh and so states are coupled. The so-hole confinement will not be dealt with.

The results from our simple model description are in excellent agreement with the results from the much more accurate Chang-Schulman analysis when our Γ -point el, hh, lh, and so effective masses are chosen in accordance with the corresponding masses in their *s,p,s** tight-binding analysis.

In the following, we discuss the el, hh, lh, and so Kane model and the problem of spurious solutions (Sec. II), the reduction of the model to the particle in the box descriptions and the lh-so Kane model (Sec. III), the comparison with the Chang-Schulman results (Sec. IV) and the problem of the choice of the effective masses when application to experimental spectra is intended (Sec. V). Results are summarized in Sec. VI.

II. KANE MODEL

We describe each constituent material of the quantum well with an eight-band Kane model. The set of Γ -point

basis states includes the s -like spin-up and spin-down conduction band states, the fourfold p -like $j = \frac{3}{2}$ valence band states and the twofold $j = \frac{1}{2}$ spin-orbit split-off valence band states. All the other bands are taken into account perturbatively using a Löwdin renormalization procedure.¹⁰ We take the quantization axis of the angular momenta to be perpendicular to the quantum well interfaces and call it the z axis. As usual we set the Kane B parameter equal to zero, since $B \neq 0$ yields only a minor k^3 contribution to the bands.¹⁰ We also disregard the k -dependent part of the spin-orbit coupling, since the corresponding term linear in k in the dispersion of the bands is extremely small.¹⁰ Inversion symmetry is then effectively restored in the materials and the eigenvalues occur in degenerate pairs, the Kramers doublets. The eight Γ -point basis states in the Kane-type $k \cdot p$ analysis then decouple into two sets of four states, i.e., the set

$$u_{el} = \left| \frac{1}{2}, \frac{1}{2} \right\rangle = |s\uparrow\rangle, \quad (1a)$$

$$u_{hh} = \left| \frac{3}{2}, \frac{3}{2} \right\rangle = \frac{1}{\sqrt{2}} |(x+iy)\uparrow\rangle, \quad (1b)$$

$$u_{lh} = \left| \frac{3}{2}, \frac{1}{2} \right\rangle = \frac{1}{\sqrt{6}} |(x+iy)\downarrow\rangle - \sqrt{\frac{2}{3}} |z\uparrow\rangle, \quad (1c)$$

$$u_{so} = \left| \frac{1}{2}, \frac{1}{2} \right\rangle = \frac{1}{\sqrt{3}} [|(x+iy)\downarrow\rangle + |z\uparrow\rangle], \quad (1d)$$

$$\underline{H}^l = \begin{vmatrix} E_g^l + s^l \hat{\epsilon} & -\sqrt{\frac{2}{3}} i P^l \hat{k} & \sqrt{\frac{1}{3}} i P^l \hat{k} & 0 \\ \sqrt{\frac{2}{3}} i P^l \hat{k} & -(\gamma_1^l + 2\gamma_2^l) \hat{\epsilon} & 2\sqrt{2} \gamma_2^l \hat{\epsilon} & 0 \\ -\sqrt{\frac{1}{3}} i P^l \hat{k} & 2\sqrt{2} \gamma_2^l \hat{\epsilon} & -\Delta^l - \gamma_1^l \hat{\epsilon} & 0 \\ 0 & 0 & 0 & -(\gamma_1^l - 2\gamma_2^l) \hat{\epsilon} \end{vmatrix}. \quad (4)$$

\hat{k} stands for $-i\partial/\partial z$, E_g^l is the gap of material l and Δ^l its spin orbit splitting. The zero of energy is at the valence-band edge in the well. The operator $\hat{\epsilon} = \hbar^2 k^2 / 2m$. The valence-band discontinuity is denoted by δE_v . The coupling between s and p_z states is described by

$$P^l = -\frac{\hbar^2}{m} \int_{\text{unit cell}} d\mathbf{r} \phi_s^l(\mathbf{r}) \frac{\partial}{\partial z} \phi_{p_z}^l(\mathbf{r}), \quad (5)$$

in self-explanatory notation. The parameters s^l , γ_1^l , and γ_2^l describe the combined effect of the free-electron term in the Kane approach and the coupling of the s states (s^l) and p states (γ_1^l and γ_2^l) to the other bands. The parameters γ_1^l and γ_2^l are modified Luttinger parameters. Their relation to the true Luttinger parameters $\gamma_{1,L}^l$ and $\gamma_{2,L}^l$,¹² is given by

$$\frac{\hbar^2}{2m} (\gamma_{1,L}^l - \gamma_1^l) = \frac{1}{3} (P^l)^2 / E_g^l, \quad (6)$$

$$\frac{\hbar^2}{2m} (\gamma_{2,L}^l - \gamma_2^l) = \frac{1}{6} (P^l)^2 / E_g^l. \quad (7)$$

We now first discuss some properties of the bulk materials. The bulk wave functions are obtained from the ansatz $F_j^l \propto e^{ikz}$, where k labels the wave functions in accordance with translational symmetry along the z direction. The energy-dispersion relation $E(k)$ then follows

and the set Ku_{el} , Ku_{lh} , Ku_{hh} , and Ku_{so} . Here K corresponds to the product of inversion ($s \rightarrow -s, p \rightarrow p$), complex conjugation, and reversion of the spin. As usual, the designations s , x , y , and z refer to the corresponding symmetry properties under operations of the tetrahedral group. For $k_x = 0$ and $k_y = 0$, the only case we deal with, we write the wave functions as

$$\psi^l = \sum_j F_j^l(z) u_j^l(\mathbf{r}), \quad (2)$$

where $u_j(\mathbf{r})$ is the periodic Bloch part and $F_j^l(z)$ describes the envelope of the wave function which is slowly varying on the scale of the lattice constant a . The designation l refers to the well material ($l=1$) or the barrier material ($l=2$). The label j runs over the states from Eq. (1) as well as over the other Γ -point states. When the effect of the latter is included in the Schrödinger equation by Löwdin renormalization we obtain

$$\{\underline{H}^l - [(l-1)\delta E_v + E] \underline{I}\} \mathbf{F}^l = 0, \quad (3)$$

where \mathbf{F}^l is the column vector $(F_1^l, F_2^l, F_3^l, F_4^l)$, \underline{I} is the unit matrix, \underline{H}^l is the matrix operator,

from the secular equation,

$$|\underline{H}^l(\hat{k} = k) - [(l-1)\delta E_v + E] \underline{I}| = 0. \quad (8)$$

The hh band is completely decoupled from the other bands and its dispersion is purely parabolic with an effective mass satisfying

$$m/m_{hh}^l = \gamma_1^l - 2\gamma_2^l. \quad (9)$$

For k near zero, the dispersion of the other bands is also parabolic and the corresponding effective masses are

$$m/m_{el}^l = s^l + \lambda^l (1 + \frac{1}{2} r^l), \quad (10)$$

$$m/m_{lh}^l = \gamma_1^l + 2\gamma_2^l + \lambda^l, \quad (11)$$

$$m/m_{so}^l = \gamma_1^l + \frac{1}{2} \lambda^l r^l, \quad (12)$$

where

$$\lambda^l = 4m(P^l)^2 / (3\hbar^2 E_g^l), \quad (13)$$

$$r^l = E_g^l / (E_g^l + \Delta^l). \quad (14)$$

It is now clear that knowledge of the four Γ -point effective masses m_{el}^l , m_{hh}^l , m_{lh}^l , and m_{so}^l , assuming E_g^l and Δ^l to be given, completely determines the four coupling parameters P^l , s^l , γ_1^l , and γ_2^l , and thus yields a unified

description of the el, hh, lh, and so bands.

In the approach of Bastard⁸ s^l , γ_1^l , and γ_2^l are set equal to zero in the el and lh band and the limit $\Delta^l \rightarrow \infty$ is taken, having materials with large spin-orbit splittings in mind. The (Γ -point) effective masses of el and lh bands are then automatically equal. Setting s^l , γ_1^l , and γ_2^l equal to zero for the case we have in mind is physically unrealistic. For example for the well material the dispersion relation of the el, lh, and so bands then becomes

$$(P^{(1)})^2 k^2 = \frac{E(E - E_g^{(1)})(E + \Delta^{(1)})}{E + \frac{2}{3}\Delta^{(1)}}, \quad (15)$$

yielding infinite k^2 values when E approaches $-\frac{2}{3}\Delta^{(1)}$. Moreover, m_{el}^l , m_{lh}^l , and m_{so}^l are determined by one parameter only, λ^l . It is easily verified that this is not consistent with the experimental values of the effective masses. Finally, setting γ_1^l and γ_2^l equal to zero in the hh band is clearly unrealistic since it yields a dispersionless hh band.

Having established a simple model for the bulk band structure as determined by the gap, the spin-orbit splitting and four effective masses, we now turn to the quantum-well problem. The envelope functions $\mathbf{F}^{(1)}$ and $\mathbf{F}^{(2)}$ must then be joined across the interfaces by suitable boundary conditions. Since we are dealing with type I quantum wells, potentials arising from charge redistribution across the interfaces will be disregarded; we work in the so-called "flat-band" approximation.¹³ From the structural similarity of the isoelectronic materials in the quantum well, the approximation is invoked in which the basis wave functions u_j^l , $j = \text{el, hh, lh, so}$, are the same in the materials 1 and 2. This then also implies $P^{(1)} = P^{(2)} = P$. Later on when s^l , P^l , γ_1^l , and γ_2^l are determined from the four given effective masses in each material we will check for the continuity of P^l .

The continuity of the u part of the wave function is actually a troublesome assumption: It cannot be correct exactly. The excellent agreement between the results from our approach, using that assumption, and the Chang-Schulman nearest-neighbor tight-binding approach, not containing the assumption, is an *a fortiori* demonstration of the usefulness of invoking the continuity of u , at least for GaAs/Ga_{1-x}Al_xAs. Our results are consistent with the outcome of a recent analysis by Zhu and Kroemer,¹⁴ who derive interface connection rules similar to ours when a nearest-neighbor tight-binding description is used for two very similar semiconductors.

Continuity of the wave function now implies

$$\mathbf{F}^{(1)} = \mathbf{F}^{(2)} \quad (16)$$

at the interfaces. The further boundary conditions on the envelope functions are obtained as follows. Equations (3) and (4), with say $l = 1$, can also be considered as the equations describing the quantum well as a whole when s , P , γ_1 , and γ_2 are considered as functions of z . For such "effective-mass-type" functions to be defined they must change slowly on the scale of the lattice parameter. At the interfaces they will change rapidly on the scale of the envelope changes. Of course the Hamilton operator \underline{H} must be suitably modified to ensure its hermiticity; cf.

Bastard.⁸ Integration across the interfaces of the resulting equations then yields

$$\underline{D}^{(1)} \frac{\partial}{\partial z} \mathbf{F}^{(1)} = \underline{D}^{(2)} \frac{\partial}{\partial z} \mathbf{F}^{(2)} \quad (17)$$

at the interfaces. The matrix \underline{D}^l is given by

$$\underline{D}^l = \begin{pmatrix} -s^l & 0 & 0 & 0 \\ 0 & \gamma_1^l + 2\gamma_2^l & -2\sqrt{2}\gamma_2^l & 0 \\ 0 & -2\sqrt{2}\gamma_2^l & \gamma_1^l & 0 \\ 0 & 0 & 0 & \gamma_1^l - 2\gamma_2^l \end{pmatrix}. \quad (18)$$

Note that for interfaces with monolayer sharpness, the approach, strictly speaking, does not hold. However, studies by Schulman¹⁵ have shown that the dependence on gradients in grading interfaces is very weak. Note also that the boundary conditions (17) are of the same type as derived by Altarelli.¹¹ However, we do not use continuity of the current to derive these conditions. The currents associated with the well part and the barrier part of a confinement state are zero because the corresponding parts of the state are real valued.

Obtaining the confinement wave functions and energies is now in principle simple. At a given energy E the dispersion relation (8) is a polynomial of degree 4 in k^2 and so it yields eight solutions, $k_\alpha^l(E)$, $\alpha = 1, \dots, 8$. The corresponding eigensolutions are $\mathbf{F}_\alpha^l(E)$. A confinement state is then formed out of the linear combination of eight well and eight barrier solutions. Equations (16) and (17) at the two interfaces determine the 16 coefficients involved in the linear combination by means of a secular equation involving a 16×16 secular matrix. Solving that equation yields the confinement states and energies.

At this stage of the discussion it is important to make two observations. First, the problem to be solved is still rather complicated. This is annoying from a physical point of view, especially since many approximations have been invoked already. Second, there is something wrong with the description given. For each energy E there are four solutions k^2 . Three of them are physically realistic and the corresponding complex band structure¹⁶ is depicted in Fig. 1 for the set of parameters to be used later on. The hh band is completely decoupled from the other bands and corresponds to imaginary k (k^2 negative) for energies above the top of the valence band. The el and lh bands are coupled across the gap by an "imaginary" band. The fourth k^2 solution, not depicted in Fig. 1, is a physically unrealistic and thereby spurious solution. Numerically it corresponds to k values outside the Brillouin zone. Basically the spurious solution has its origin in the incompleteness of the set of basis functions in the Kane approach, which makes it impossible to satisfy the periodicity relation $E(k) = E(k + 2\pi n/a)$ in the Brillouin zone; a is the lattice constant, $n = 0, 1, 2, \dots$. The spurious solution corresponds to a solution outside the Brillouin zone which is not, but should actually be, a periodic continuation of the solution inside the Brillouin zone. The problem is now that the spurious solutions are taken completely seriously in the construction of the confinement wave functions as given before. Although this may not be

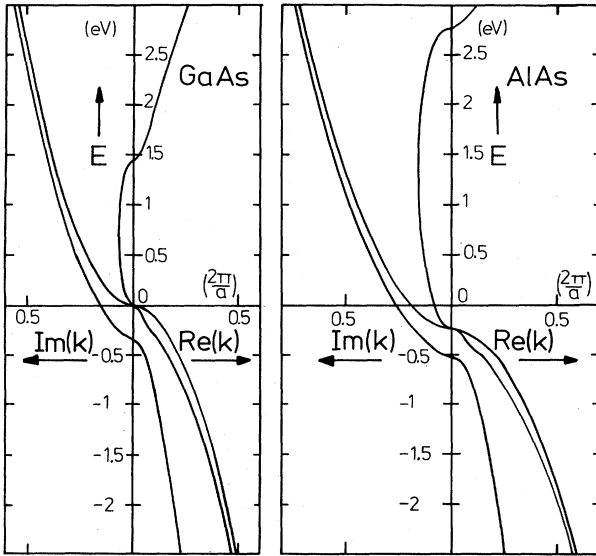


FIG. 1. Complex band structure of GaAs and AlAs describing energy E versus complex k perpendicular to the quantum-well interfaces as calculated from Eq. (8) using the parameters of Table I.

of significant influence on the confinement energies and states finally obtained, it seems at least dangerous to base the calculations on a model containing physically unrealistic solutions. In view of these observations, i.e., the lack of simplicity and the presence of spurious solutions, we propose much more simple and physically realistic models in the next section.

The spurious solutions are related to the wing-band solutions discussed by White and Sham.⁷ Both types of solutions correspond to k^2 values outside the Brillouin zone. However, the wing-band solutions are rapidly decaying whereas the spurious solutions are oscillatory in nature. In contrast to the oscillatory solutions, the decaying ones do not strongly influence the determination of confinement energies. However, the two-band, electron-light-hole-type, Kane matrix proposed by White and Sham⁷ is not consistent with the actual matrix appearing in a Kane-type description of GaAs in the limits $\Delta=0$ and $\Delta=\infty$. This is easily verified tracing back the origin of the modified Luttinger parameters in the two-band model. The actual two-band matrix for GaAs (or AlAs) does yield spurious- and not wing-band solutions.

III. SIMPLE MODELS FOR CONFINEMENT

The hh band is completely decoupled from the other bands. According to Eqs. (3) and (4), the heavy holes satisfy a particle in the box description according to

$$\left[-\frac{\hbar^2}{2m_{hh}^l(E)} \frac{\partial^2}{\partial z^2} - (l-1)\delta E_v - E \right] F_{hh}^l(z) = 0, \quad (19)$$

with the boundary conditions

$$F_{hh}^{(1)} = F_{hh}^{(2)}, \quad (20)$$

$$\frac{1}{m_{hh}^{(1)}(E)} \frac{\partial}{\partial z} F_{hh}^{(1)} = \frac{1}{m_{hh}^{(2)}(E)} \frac{\partial}{\partial z} F_{hh}^{(2)} \quad (21)$$

at the two interfaces. Equation (21) follows from (19) by means of direct integration across the interfaces as described in the preceding section.

Since the gaps in the well and the barrier material are large compared to the confinement energies, it seems reasonable to hope that a separate description of electrons and (lh + so) holes is possible. For the electrons one may then also take a particle in the box description according to

$$\left[-\frac{\hbar^2}{2m_{el}^l(E)} \frac{\partial^2}{\partial z^2} + E_g^l - (l-1)\delta E_v - E \right] F_{el}^l(z) = 0, \quad (22)$$

with the boundary conditions

$$F_{el}^{(1)} = F_{el}^{(2)}, \quad (23)$$

$$\frac{1}{m_{el}^{(1)}(E)} \frac{\partial}{\partial z} F_{el}^{(1)} = \frac{1}{m_{el}^{(2)}(E)} \frac{\partial}{\partial z} F_{el}^{(2)}. \quad (24)$$

The energy-dependent effective mass $m_{el}^l(E)$ is chosen in such a way that

$$E - E_g^l + (l-1)\delta E_v = \frac{\hbar^2 k^2}{2m_{el}^l(E)}, \quad (25)$$

where, for a given energy E , the wave vector k is chosen to be on the (complex) electron branch of Fig. 1. One may actually "derive" Eq. (22) from Eqs. (3) and (4). For E close to $E_g^{(1)}$, we may disregard the terms involving γ_1^l and γ_2^l compared to E , or better still, replace k^2 in these terms by an energy-dependent expression in accordance with Eq. (25). The envelope functions F_{lh} and F_{so} may then be eliminated and we end up with Eq. (22). Note that this procedure implies that the dominant contribution to the column vector (F_{el}, F_{lh}, F_{so}) is of the form $\exp(\pm ikz)$, where $k^2(E)$ describes the electron branch of Eq. (25). In the next section we will see that Eqs. (22)–(24) provide an excellent description for the electron confinement states.

The description of the lh confinement states is more complicated. The confinement potential step may be comparable to the spin-orbit splitting. An example is GaAs/AlAs (see the next section). The confinement energies may then also be comparable to the spin-orbit splittings and so the lh-so coupling cannot be disregarded. The question is then how to cope with this problem without having to deal with a spurious solution. We must realize that the parameters s^l , γ_1^l , and γ_2^l , describing the effects of bands not explicitly described in the model, strictly speaking, depend on energy. The Löwdin renormalization gives expressions for them with an energy-dependent denominator, such as $E - E_c^l$ for s^l , ignoring the free-electron part. Here E_c^l is the energy of the Γ_{15} state closest to the conduction band edge. For $E = E_g^l + (l-1)\delta E_v$ we find the expression usually quoted¹⁰ and which is a good approximation for energies close to the conduction band edge. For E close to the valence band edge s^l will be considerably smaller. However, for such energies the dispersion relation is not sensitive to the value of s^l . This is understandable as $-s^l \hat{e}$ is then much smaller than $E_g^l - E$. We have numerically verified that this is indeed true for the examples we have studied. An

ultimate consequence of this is that we may put $s^l=0$ when we are interested in the determination of the hole confinement energies. The envelope function F_{el}^l may then be eliminated from Eqs. (3) and (4) and we end up with

$$\{\underline{G}^l - [(l-1)\delta E_v + E]\underline{I}\} \mathbf{f}^l = 0, \quad \mathbf{f}^l = \begin{pmatrix} F_{lh}^l \\ F_{so}^l \end{pmatrix}, \quad (26)$$

where

$$\underline{G}^l = \begin{vmatrix} -a^l \hat{\epsilon} & c^l \hat{\epsilon} \\ c^l \hat{\epsilon} & -b^l \hat{\epsilon} - \Delta^l \end{vmatrix}, \quad (27)$$

and the quantities a^l , b^l , and c^l are given by

$$a^l = \frac{1}{2} \gamma_1^l + \gamma_2^l + \Pi^l, \quad (28)$$

$$b^l = (\gamma_1^l + \Pi^l) / 2, \quad (29)$$

$$c^l = (2\gamma_2^l + \Pi^l) / \sqrt{2}, \quad (30)$$

where Π^l depends on energy according to

$$\Pi^l = 2mP^2 / \{3\hbar^2 [E_g^l - (l-1)\delta E_v - E]\}. \quad (31)$$

The dispersion relation as given by

$$\|\underline{G}^l - [(l-1)\delta E_v + E]\underline{I}\| = 0 \quad (32)$$

now describes the lh and so band dispersion, and, being of the second order in k^2 , contains no spurious solution. Along the lines described in the preceding section we derive the continuity relations

$$\mathbf{f}^{(1)} = \mathbf{f}^{(2)}, \quad (33)$$

$$\underline{A}^{(1)} \frac{\partial}{\partial z} \mathbf{f}^{(1)} = \underline{A}^{(2)} \frac{\partial}{\partial z} \mathbf{f}^{(2)}, \quad (34)$$

where the matrix \underline{A}^l is given by

$$\underline{A}^l = \begin{vmatrix} -a^l & c^l \\ c^l & -b^l \end{vmatrix}. \quad (35)$$

This leaves us with a simple description of lh confinement involving no spurious solutions.

When the confinement potential step of the light holes is considerably smaller than the spin-orbit splittings, the confinement energies will also be smaller than these splittings. In the next section we will see that examples are furnished by GaAs/Ga_{1-x}Al_xAs with $x \leq 0.4$. A treatment similar to that of the electrons is then possible, i.e., the Eqs. (22)–(24) with el replaced by lh, and where $m_{lh}^l(E)$ satisfies

$$E + (l-1)\delta E_v = -\frac{\hbar^2 k^2}{2m_{lh}^l(E)}, \quad (36)$$

for a given E the wave vector k is chosen to be on the (complex) lh branch of Fig. 1.

The confinement energies resulting from the particle in the box descriptions for $\alpha = el, lh, \text{ or } hh$ are well known to be given by

$$\cos(k_\alpha^{(1)} w) + \frac{1}{2} \left[\xi_\alpha - \frac{1}{\xi_\alpha} \right] \sin(k_\alpha^{(1)} w) = 0, \quad (37)$$

where

$$\xi_\alpha(E) = k_\alpha^{(2)} m_\alpha^{(1)} / k_\alpha^{(1)} m_\alpha^{(2)}. \quad (38)$$

$k_\alpha^l(E)$ is the α -branch solution of Eq. (8) (Fig. 1) and $m_\alpha^l(E)$ follows from Eqs. (9), $\alpha = hh$, (25), $\alpha = el$, and (36), $\alpha = lh$. The well width is denoted by w .

When the lh and so bands are coupled according to Eq. (26), the evaluation of the lh confinement states is a bit more complicated. As an example we evaluate the even confinement states. For a given value of E , let Eq. (26) be solved by $(k_j^l)^2$ ($j=1,2$) and $\mathbf{f}_j^l = \mathbf{v}_j^l$. Define $k_j^l = (|k_j^l|^2)^{1/2}$ and let $(k_1^l)^2 < (k_2^l)^2$. An even confinement state is then described in the well ($-w/2 \leq z \leq w/2$) by

$$\mathbf{F} = a_1^{(1)} \cosh(k_1^{(1)} z) \mathbf{v}_1^{(1)} + a_2^{(1)} \cos(k_2^{(1)} z) \mathbf{v}_2^{(1)} \quad (39)$$

and in the barrier ($z > w/2$) by

$$\mathbf{F} = \sum_{j=1,2} a_j^{(2)} e^{-k_j^{(2)} z} \mathbf{v}_j^{(2)}. \quad (40)$$

Substitution into the boundary conditions (33) and (34) determines the four coefficients a_j^l and the confinement energy. For odd confinement states the procedure is easily modified.

We have now arrived at a simple and unified description of el, hh, and lh confinement. The unification is important for the determination of energies or wavelengths of transition between electron and hole confinement states. Separate adjustments of parameters for electron and hole states may yield bad transition wavelengths, especially when the nonparabolicity of the bands becomes important.

IV. NUMERICAL RESULTS

We are now going to apply our simple model to a GaAs/Ga_{1-x}Al_xAs quantum well and to compare the results for confinement states with those from the Chang and Schulman (CS) approach.⁴ These authors have optimized⁶ their tight-binding parameters, not only with respect to certain energies in the band structure but also in such a way that a certain given set of Γ -point el, hh, lh, and so effective masses is reproduced well in GaAs and AlAs. The two sets of effective masses are given in Table I. Using our Kane description we have calculated from these masses the sets s^l , γ_1^l , γ_2^l , and P^l , $l=1,2$. They are also given in Table I. We note that in line with our assumptions the parameter P^l is approximately the same in the well and the barrier. The dispersion relation obtained from our Kane analysis is in excellent agreement with the CS dispersion, as is shown in Fig. 2. More precisely, for electron confinement energies less than 300 meV and hole confinement energies less than 200 meV, the difference in dispersion can rarely be of influence on the differences in confinement energies to be obtained from the CS and our approach.

The comparison of confinement energies is done for GaAs/AlAs and GaAs/Ga_{0.64}Al_{0.36}As. The quantum-well GaAs/AlAs provides a severe test of our model in view of the large confinement potentials for the electrons (1.36 eV) and for the light and heavy holes (0.236 eV); cf. Table I. For the electrons we restrict ourselves to confinement energies below 300 meV since otherwise admixtures with the X state in AlAs will occur. As Fig. 3 shows, the

TABLE I. Gaps, spin-orbit splittings, effective masses, and input coupling parameters to the Kane model.

	E_g (eV)	Δ (eV)	m_{el}/m	m_{hh}/m	m_{lh}/m	m_{so}/m	$\frac{4}{3} \frac{m}{\hbar^2} p^2$ (eV)	s	γ_1	γ_2
GaAs	1.430	0.343	0.067	0.454	0.070	0.143	18.80	-3.52	1.67	-0.26
AlAs	3.002	0.281	0.222	0.751	0.150	0.267	17.66	-4.07	1.06	-0.14
Ga _{0.64} Al _{0.36} As	1.995	0.320	0.107	0.535	0.099	0.188	18.84	-4.16	1.27	-0.30

CS results for the confinement energies¹⁷ are reproduced to an accuracy of 3% for the electrons, 2% for the heavy holes, and 5% for the light holes in the lh-so coupling model. It is seen that the lh particle in the box description is worse than the lh-so coupling model. This is to be expected since spin-orbit splittings and hole confinement potential are of comparable magnitude, cf. Table I. Our simple model does not describe the coupling between the second hh confinement state and the first light-hole confinement state as observed by Chang and Schulman.¹⁸ This occurs for well widths around 90 Å. The relative errors obtained are then slightly larger than 5%. We expect the results for well widths above 100 Å to be equally good

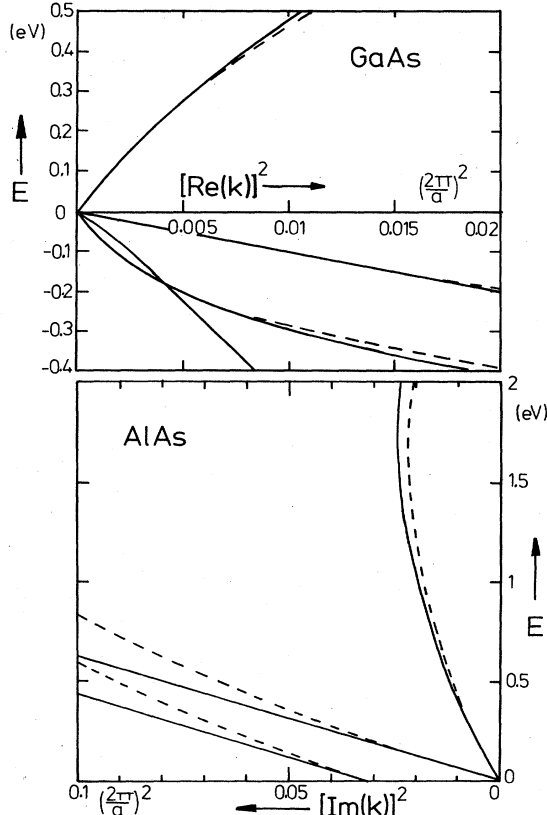


FIG. 2. Band structure energies E of GaAs and AlAs versus k^2 as calculated from Eq. (8) using the parameters of Table I. The bands shown are the relevant ones for the construction of the well and barrier wave functions. In GaAs, this means real k values. In AlAs imaginary k values. The bands in GaAs are shifted in energy so that the $k=0$ energies are at the zone center. The dashed lines are calculated using the Chang-Schulman tight-binding analysis (Ref. 6).

when we restrict ourselves to the energy ranges discussed earlier. For GaAs/Ga_{0.64}Al_{0.36}As, our confinement energies compare even more favorably with the CS energies. All relevant parameters of Ga_{0.64}Al_{0.36}As are listed in Table I. The gap, spin-orbit splitting, and the effective masses are taken from the CS code. We note that m_{el} and m_{hh} do not interpolate linearly with the Al concentration

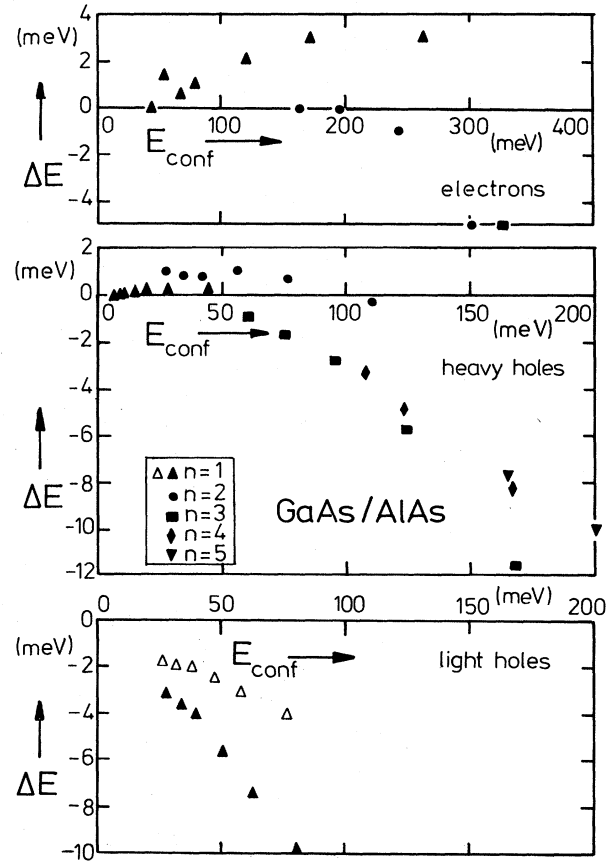


FIG. 3. Difference ΔE in the confinement energy obtained from the extensive Chang-Schulman tight-binding analysis and the confinement energy as calculated from the simple theory presented in this paper is plotted versus the latter confinement energy. The specific points correspond to a quantum well consisting of 10, 14, 18, ..., 34 monolayers of GaAs cladded by AlAs. The various closed symbols refer to different n quantum numbers of confinement states considered, and the simple theory refers to a particle in the box description with a well-chosen energy dependent effective mass. The open symbols refer to $n=1$ light-hole confinement energies as calculated from a simple model in which only the coupling between light holes and spin-orbit split-off holes is retained.

x . The hole confinement potential (0.085 eV) is now considerably less than the spin-orbit splittings. We expect the lh particle in the box description to be appropriate. In contrast to AlAs, Ga_{0.64}Al_{0.36}As is (barely) direct. This means that only for electron states very close in energy to the top of the potential well (480 meV) the X minimum of the barrier material will be involved in the el-confinement states. The CS results for the confinement energies are reproduced to an accuracy of 3% for the electrons, 1% for the heavy holes, and 2% for the light-hole particle in the box model. The lh-so coupled model gives slightly worse results in the latter case.

The energies or wavelengths corresponding to transitions between electron and light or heavy hole confinement states are accurate to 0.5% for confinement energies in the range of up to 300 meV for the electrons and 200 meV for the holes. For well widths smaller than ≈ 10 monolayers the CS approach, as well as our approach, may not be very accurate. The relative importance of the interfaces increases with a decreasing number of monolayers in the well. The particular approximations involved in the description of the atoms at the interfaces in the CS tight-binding approximation then begin to play an important part. It is also hard to visualize our simple-envelope-function-type description still working for wells that are that thin.

V. APPLICATION TO EXPERIMENTS

The application of our simple model to describe experimental absorption or luminescence spectra of GaAs/Ga_{1-x}Al_xAs quantum wells requires an accurate knowledge of the Γ -point el, hh, lh, and so effective masses as well as of the electron and hole confinement potentials. For GaAs, the information on the effective masses is available with reasonable accuracy, but for AlAs the situation is worse. Different from GaAs, the el, hh, and lh bands in AlAs are anisotropic around the Γ points. Experimental determinations¹⁹ have yielded directionally averaged effective masses, but we need the effective masses along the [100] direction. Theoretical evaluations yield conflicting results.²⁰⁻²³ The set of effective mass parameters used by Chang and Schulman, and in this paper, is based on the theoretical work of Lawaetz.²¹ More recent work of Hess *et al.*²³ yields a completely different set: $m_{el}=0.15$, $m_{hh}=0.48$, $m_{lh}=0.21$, and $m_{so}=0.30$ for AlAs. Fortunately the dependence of the confinement energies on the barrier effective masses is rather weak. We have estimated this dependence from particle in the box descriptions with constant effective masses. For the $n=1$ confinement levels we find $(\Delta E_{\text{conf}}/E_{\text{conf}})/(\Delta m/m)$ to be ≈ -0.2 for the electrons and heavy holes and ≈ -0.3 for the light holes. The higher confinement levels appear to be a factor of 2 less sensitive to the barrier effective mass. The estimate applies both to GaAs/AlAs and GaAs/Ga_{0.64}Al_{0.36}As. For GaAs/AlAs, the Hess set yields 6% lower el and hh confinement energies and 12% higher lh confinement energies than the Lawaetz set. This effect is certainly much bigger than the inaccuracy due to the simplification in our approach as compared to that of Chang and Schulman. At present, we

are clearly no longer limited by inaccuracies in the theoretical description but by the lack of knowledge of effective masses in the barrier material.

An energy-dependent effective mass in the well has been introduced earlier by Kolbas²⁴ and used by Vojak *et al.*³ to interpret luminescence spectra. Kolbas's $m_{el}(E)$ is an optical effective mass, i.e., a mass weighted with the Fermi-Dirac distribution, as described by Cardona.²⁵ This is not the energy-dependent effective mass that should be used in a calculation of confinement energies. However, we note that the dispersion $E(k)$ corresponding to Kolbas's $m_{el}(E)$ only starts to deviate from the CS dispersion for energies larger than 200 meV above the conduction-band edge.

The confinement potentials in GaAs/Ga_{1-x}Al_xAs quantum wells are commonly taken according to the 85/15 rule: the conduction- and valence-band edge discontinuities are 85% and 15% of the gap difference, respectively. The rule is based on Dingle's¹ analysis of experimental spectra using a particle in the box description with constant effective masses and invoking the incorrect continuity of the derivative of the envelope function. Direct measurements using core level spectroscopy²⁶ lack the precision to test the rule, as does the theoretical work.²⁷ Very recent experiments by Miller *et al.*,²⁸ Watanabe *et al.*²⁹ and Dawson *et al.*³⁰ provided evidence for ratios considerably smaller than 85/15.

A further complication in the comparison of experimental and "theoretical" luminescence spectra arises from the two-particle effects giving rise to bound and free excitons.³¹ We feel that the present knowledge in this field³² no longer limits the comparison, at least not for the lowest confinement energies.

VI. CONCLUSIONS

We have presented simple particle in the box descriptions for a calculation of the confinement energies in a GaAs/AlAs-type quantum well. Energy-dependent effective masses determined from a Kane-type description of the well and barrier material have been used. In each material the four Kane coupling parameters are adjusted to the el, hh, lh, and so Γ -point effective masses. This leads to a unified description of el, hh, lh, and so dispersion. For hole confinement potentials close to the spin-orbit splitting, we have used a model in which the lh and so bands are coupled along the lines of the Kane model.

Our confinement energies are in excellent agreement with those obtained from the Chang-Schulman 20-band tight-binding approach; accuracies have been described in Sec. III. It should be stressed that the Chang-Schulman approach has many more potential capabilities. For example, it is capable of describing the $n=2$ hh and $n=1$ lh coupling¹⁸ and the admixture of Ga_{1-x}Al_xAs X -point derived states when the confinement energies approach that point.

The virtue of our analysis lies in its simplicity, making it directly available to any experimental physicist dealing with quantum wells. The accuracy is at present mainly

limited by the lack of knowledge of barrier (AIA) effective masses. Experiments to determine these quantities, for example along the lines of cyclotron resonance, are thus called for.

ACKNOWLEDGMENTS

The authors are grateful to Dr. Chang and Dr. Schulman for putting their tight-binding code for superlattices at their disposal.

- ¹R. Dingle, in *Festkörperprobleme*, Vol. XV of *Advances in Solid State Physics* (Pergamon, New York, 1975), p. 21.
- ²D. Mukherji and B. R. Nag, *Phys. Rev. B* **12**, 4338 (1975).
- ³B. A. Vojak, W. D. Laidig, N. Holonyak, Jr., M. D. Camras, J. J. Coleman, and P. D. Dapkus, *J. Appl. Phys.* **52**, 621 (1981).
- ⁴J. N. Schulman and Y. C. Chang, *Phys. Rev. B* **24**, 4445 (1981); Y. C. Chang and J. N. Schulman, *J. Vac. Sci. Technol.* **21**, 540 (1982).
- ⁵P. Vogl, H. P. Hjalmarson, and J. D. Dow, University of Illinois at Urbana-Champaign Report (unpublished).
- ⁶J. N. Schulman and Y. C. Chang, *Phys. Rev. B* **31**, 2056 (1985).
- ⁷S. R. White and L. J. Sham, *Phys. Rev. Lett.* **47**, 879 (1981).
- ⁸G. Bastard, *Phys. Rev. B* **24**, 5693 (1981).
- ⁹G. Bastard, *Phys. Rev. B* **25**, 7584 (1982).
- ¹⁰E. O. Kane, in *Handbook on Semiconductors* (North-Holland, New York, 1982), Vol. I, p. 193.
- ¹¹M. Altarelli, *Phys. Rev. B* **28**, 842 (1983); *Physica* **117&118B**, 747 (1983).
- ¹²J. M. Luttinger, *Phys. Rev.* **102**, 1030 (1956).
- ¹³L. J. Sham and M. Nakayama, *Phys. Rev. B* **20**, 734 (1979).
- ¹⁴QI-GaO Zhu and H. Kroemer, *Phys. Rev. B* **27**, 3519 (1983).
- ¹⁵J. N. Schulman, *J. Vac. Sci. Technol. B* **1**, 644 (1983).
- ¹⁶V. Heine, *Proc. Phys. Soc. London* **81**, 300 (1963); Y. C. Chang, *Phys. Rev. B* **25**, 605 (1982); Y. C. Chang and J. N. Schulman, *ibid.* **25**, 3975 (1982).
- ¹⁷We have used the numerical code developed by Chang and Schulman for superlattices (Ref. 4). The comparison with our quantum-well results was achieved by taking in the superlattice approach thick-barrier materials (≈ 40 monolayers; larger numbers yield numerical difficulties) and evaluating the superlattice energies at the superlattice wave number $q = \pi/d$, where $q = 2\pi/d$ corresponds to the superlattice Brillouin zone edge. The latter procedure assures a close connection between quantum well and superlattice energies even if there is a finite amount of dispersion in the superlattice energies.
- ¹⁸Y. C. Chang and J. N. Schulman, *Appl. Phys. Lett.* **43**, 536 (1983).
- ¹⁹W. P. Dumke, M. R. Lorenz, and G. D. Pettit, *Phys. Rev. B* **5**, 2978 (1972).
- ²⁰D. J. Stukel and R. W. Euwema, *Phys. Rev.* **188**, 1193 (1969).
- ²¹P. Lawaetz, *Phys. Rev. B* **4**, 3460 (1971).
- ²²R. Braunstein and E. O. Kane, *Phys. Chem. Solids* **23**, 1423 (1962).
- ²³E. Hess, H. Neumann, and I. Topol, *Phys. Status Solidi B* **55**, 187 (1973).
- ²⁴R. M. Kolbas, Ph.D. thesis, University of Illinois at Urbana-Champaign, 1979.
- ²⁵M. Cardona, *Phys. Rev.* **121**, 752 (1961).
- ²⁶J. R. Waldrop, S. P. Kowalezyk, R. W. Grant, E. A. Krant, and D. L. Miller, *J. Vac. Sci. Technol.* **19**, 573 (1981).
- ²⁷W. R. Frensley and H. Kroemer, *Phys. Rev. B* **16**, 2642 (1977); A. D. Katnani and G. Margaritondo, *J. Appl. Phys.* **54**, 2522 (1983).
- ²⁸R. C. Miller, D. A. Kleinman, and A. C. Gossard, *Phys. Rev. B* **29**, 7085 (1984).
- ²⁹M. O. Watanabe, J. Yoshida, M. Mashita, T. Nakanisi, and A. Hojo, in *Extended Abstracts of the 16th International Conference on Solid State Devices and Materials, Kobe* (Japan Society of Applied Physics, Tokyo, 1984), p. 181.
- ³⁰P. Dawson, G. Duggan, H. I. Ralph, K. Woodbridge, and G. W. 't Hooft, *Superlattices Microstruct.* **1**, 231 (1985).
- ³¹B. A. Vojak, N. Holonyak, Jr., W. D. Laidig, and K. Hess, *Solid State Commun.* **35**, 477 (1980); R. C. Miller, A. C. Gossard, W. T. Tsang, and O. Munteanu, *ibid.* **43**, 519 (1982).
- ³²G. Bastard, E. E. Mendez, L. L. Chang, and L. Esaki, *Phys. Rev. B* **26**, 1974 (1982); C. Mailhot, Y. C. Chang and T. C. McGill, *ibid.* **26**, 4449 (1982); R. L. Greene and K. K. Bajaj, *Solid State Commun.* **45**, 825 (1983); **45**, 831 (1983).